

Resubmitted to the *Astrophysical Journal*

Molecular line opacity of LiCl in the mid-infrared spectra of brown dwarfs

P. F. Weck

*Department of Chemistry, University of Nevada Las Vegas,
4505 Maryland Parkway, Las Vegas, NV 89154-4003*

`weckp@unlv.nevada.edu`

A. Schweitzer

*Hamburger Sternwarte, Universitaet Hamburg,
Gojenbergsweg, D-21029 Hamburg, Germany*

`Andreas.Schweitzer@hs.uni-hamburg.de`

K. Kirby

*Institute for Theoretical Atomic, Molecular & Optical Physics,
Harvard-Smithsonian Center for Astrophysics, 60 Garden Street, Cambridge, MA 02138*

`kkirby@cfa.harvard.edu`

P. H. Hauschildt

*Hamburger Sternwarte, Universitaet Hamburg,
Gojenbergsweg, D-21029 Hamburg, Germany*

`yeti@hs.uni-hamburg.de`

P. C. Stancil

*Department of Physics and Astronomy and Center for Simulation Physics,
The University of Georgia, Athens, GA 30602-2451*

`stancil@physast.uga.edu`

ABSTRACT

We present a complete line list for the $X^1\Sigma^+$ electronic ground state of $^7\text{Li}^{35}\text{Cl}$ computed using fully quantum-mechanical techniques. This list includes transition energies and oscillator strengths in the spectral region $0.3 - 39,640.7 \text{ cm}^{-1}$ for all allowed rovibrational transitions in absorption within the electronic ground state. The calculations were performed using an accurate hybrid potential constructed from a spectral inversion fit of experimental data and from recent multi-reference single- and double-excitation configuration interaction calculations. The line list was incorporated into the stellar atmosphere code **PHOENIX** to compute spectra for a range of young to old T dwarf models. The possibility of observing a signature of LiCl in absorption near $15.8 \mu\text{m}$ is addressed and the proposal to use this feature to estimate the total lithium elemental abundance for these cool objects is discussed.

Subject headings: molecular data — stars: atmospheres — stars: late-type

1. Introduction

In the study of low-mass stellar objects, the presence or absence of the Li I 6708 Å resonance line has played an important role in ascertaining whether the object is a brown dwarf. However, the use of this so-called *lithium test* (Rebolo, Martin, & Magazzu 1992) to determine substellarity has some drawbacks. L dwarfs which lie just below the bottom or at the edge of the hydrogen-burning main-sequence may have some period in their early evolution of lithium burning, depleting their lithium abundance, decreasing the strength of the Li I resonance line, and thereby suggesting they are main-sequence stars. Furthermore, the depletion of lithium is age dependent, which in turn can be used as a clock under the correct conditions (see e.g. Basri, Marcy & Graham 1996; Chabrier, & Baraffe 1997; Barrado y Navascués, Stauffer & Patten 1999, and references therein). The reduction of the strength of the Li I resonance line can also occur in lower temperature objects ($T_{\text{eff}} < 1500 \text{ K}$), near the L/T dwarf interface, due to the sequestering of lithium into molecular species such as LiCl, LiH, and LiOH (Lodders 1999). In either case, conclusions drawn from the lithium test alone (like age determination, or substellarity in the case of L dwarfs) may be inaccurate.

Thermochemical equilibrium calculations of cool dwarf atmospheres (Lodders 1999) suggest that LiCl is the dominant Li-bearing gas over an extended domain of the temperature-pressure diagram. LiCl has a large dipole moment in its ground electronic state which may give rise to an intense rovibrational line spectrum in the mid-infrared near $15.8 \mu\text{m}$. As such, LiCl may give a significant absorption feature in L and T dwarf spectra as suggested by Lodders (1999) and Burrows, Marley & Sharp (2000). If the feature is observable, it could

be used to estimate the total lithium elemental abundance in conjunction with optical Li I observations, to confirm the equilibrium lithium chemistry models, and to provide a better test of substellarity for cool objects.

In this work, we continue our long term project to update and complete molecular opacity data (Weck et al. 2003a,b; Weck, Stancil & Kirby 2003c; Weck, Kirby & Stancil 2004). Here we present a complete line list (transition energies and oscillator strengths) of all allowed rovibrational transitions in the electronic ground state of ${}^7\text{Li}^{35}\text{Cl}$. The calculations were performed using an accurate hybrid potential and the dipole moment function of Weck et al. (2004). The line list was incorporated into the stellar atmosphere code PHOENIX (Hauschildt & Baron 1999) to compute spectra for a range of T dwarf models to explore the possibility of observing LiCl.

2. Molecular calculations

For the present calculations, an accurate hybrid potential was constructed for the $X\ ^1\Sigma^+$ electronic state from the spectral inversion fit of Ogilvie (1992) and from the multi-reference single- and double-excitation configuration interaction (MRSDCI) calculations of Weck et al. (2004). The fit to the effective potential energy proposed by Ogilvie (1992) consisted of a sum of five radial functions accounting empirically for vibrational adiabatic and nonadiabatic effects. The coefficients of this expansion were determined by direct spectral inversion from the frequencies of 2577 known transitions in the infrared and microwave spectral regions for the isotopic variants ${}^6\text{Li}^{35}\text{Cl}$, ${}^6\text{Li}^{37}\text{Cl}$, ${}^7\text{Li}^{35}\text{Cl}$ and ${}^7\text{Li}^{37}\text{Cl}$. The normalized standard deviation of the fit was 0.993 over the complete domain of definition of the radial functions, i.e. for internuclear distances from $R = 3.25$ to $4.80\ a_0$. A shift in energy of -467.209627 a.u. was applied to the Ogilvie fit, in addition to a shift of $+0.0138\ a_0$ from its original equilibrium geometry, to obtain coincidence with the *ab initio* energy minimum at $R_e = 3.8185\ a_0$ determined by cubic spline interpolation from the MRSDCI data of Weck et al. (2004). Beyond the range $3.25 \leq R \leq 4.80\ a_0$, a spline fit to the *ab initio* data was used, connecting smoothly with the shifted Ogilvie fit. For internuclear distances $R > 50.0\ a_0$, a fit to the multi-reference potential has been performed using the usual van der Waals dispersion expansion to account for the long-range interaction. To our knowledge, no data have been reported for the van der Waals coefficients of the $X\ ^1\Sigma^+$ state of LiCl, thus theoretical estimates were obtained using average values from several techniques in a similar way as in Weck et al. (2003c).

In order to determine the spectroscopic constants of the $X\ ^1\Sigma^+$ potential, the vibrational wave functions, $\chi_v(R)$, and energy eigenvalues, $G(v)$, have been calculated by solving with

Numerov techniques (Cooley 1961) the radial nuclear Schrödinger equation,

$$\left[-\frac{1}{2\mu} \frac{d^2}{dR^2} + E_{el}(R) + \frac{J(J+1)}{2\mu R^2} - G(v) \right] \chi_v(R) = 0, \quad (1)$$

where μ is the reduced mass of the system, J is the rotational quantum number corresponding to the angular momentum of nuclear rotation, and $E_{el}(R)$ is the electronic potential energy. The reduced mass adopted for ${}^7\text{Li}^{35}\text{Cl}$ was $5.8435744 \text{ u}^1 = 10,651.3431 \text{ a.u.}$ (Huber & Herzberg 1979). Calculations were performed on a grid with stepsize $1 \times 10^{-3} a_0$ for the integration, over a range of internuclear distances from $R = 2.5 a_0$ to $100.0 a_0$.

The calculations yielded for this hybrid potential an energy difference $D_e = G(v_{max}) = G(141) = 4.962 \text{ eV} = 0.182 \text{ a.u.}$ and a dissociation energy $D_0 = 4.922 \text{ eV} = 0.181 \text{ a.u.}$, slightly larger than the thermochemical value, $D_0 = 4.85 \text{ eV}$, of Brewer & Brackett (1961) or the flame photometry measurement, $D_0 = 4.79 \text{ eV}$, of Bulewicz, Phillips & Sugden (1961). The introduction of the spin-orbit interaction in our calculations would lower the dissociation asymptote of the $X \ ^1\Sigma^+$ state, thereby bringing the theoretical dissociation energy into closer agreement with the experimental estimates. Our theoretical vibrational constants $\omega_e = 642.97 \text{ cm}^{-1}$, $\omega_e x_e = 4.49 \text{ cm}^{-1}$ and $\omega_e y_e = 0.02 \text{ cm}^{-1}$ are in excellent agreement with the accurate Dunham constants $Y_{10} = 642.95813 \text{ cm}^{-1}$, $-Y_{20} = 4.475085 \text{ cm}^{-1}$ and $Y_{30} = 0.0208072 \text{ cm}^{-1}$, respectively, derived from experiment by Thompson et al. (1987) for ${}^7\text{Li}^{35}\text{Cl}$. The frequency of the first band, $\nu(1-0) = \Delta G_{1/2} = 634.06 \text{ cm}^{-1}$, essentially reproduces the value of 634.076 cm^{-1} , obtained using the Dunham terms given above.

The line oscillator strengths, $f_{v'J',v''J''}^{ab}$, from rovibrational states $v''J''$ to final state $v'J'$ were computed using the $X \ ^1\Sigma^+$ dipole moment function of Weck et al. (2004) for all allowed absorption transitions between the 29,370 rovibrational levels solutions of Eq. (1), thus giving a total of 3,357,811 lines². A standard expression for the line oscillator strength can be found, for example, in Skory et al. (2003). Computed line oscillator strengths and transition energies are reported in Table 1, along with the high resolution measurements of Jones & Lindenmayer (1987), for the R -branch ($\Delta J = J' - J'' = +1$) of the fundamental vibrational band ($\Delta v = v' - v'' = +1$), for $v'' = 0$ to 4. The agreement is excellent, with a maximum transition energy discrepancy of $\sim 0.32 \text{ cm}^{-1}$ for the $R(58)$ line of the $1-0$ band.

In Figure 1, representative LiCl opacities, absorption cross section per molecule, are presented for pressures and temperature appropriate to T dwarfs. The opacities are computed using Eq. (6) of Dulick et al. (2003), using Einstein A-coefficients from the above line

¹In atomic mass units, Aston's scale

²The complete list of ${}^7\text{Li}^{35}\text{Cl}$ oscillator strength data is available online at the UGA Molecular Opacity Project database website <http://www.physast.uga.edu/ugamop/>

lists, and multiplying by a Lorentzian line profile. The full width half maximum line width is estimated by only considering collisional broadening and is typically $\sim 0.1 \text{ cm}^{-1}$ at 100 atm. The rovibrational levels of LiCl are assumed to be in equilibrium and a correction for stimulated emission is included. The fundamental and first two vibrational overtone bands, as well as a portion of the pure rotational band, are depicted. The fundamental band, with a band origin at $15.8 \mu\text{m}$, is the dominant LiCl opacity source in the mid-infrared. We note, however, that PHOENIX uses molecular line lists instead of pre-computed opacity tables as described below.

3. PHOENIX synthetic spectra

The atmosphere models used for this work were calculated as described in Allard et al. (2001). These models and their comparisons to earlier versions were the subject of a previous publication (Allard et al. 2001) and we thus do not repeat the detailed description of the models here. However, we will briefly summarize the major physical properties. The models are based on the Ames H₂O and TiO line lists by Partridge & Schwenke (1997) and Schwenke (1998) and also include the line lists for FeH by Phillips & Davis (1993) and for VO and CrH by R. Freedman (NASA-Ames, private communication). We try as much as possible to constantly add new opacities as they become available (see for example, Weck et al. 2003a,b) and the new FeH and CrH opacities recently calculated in Burrows et al. (2002) and Dulick et al. (2003) will soon be added to our database. However, as can be seen from these references, the new line lists calculated for FeH and CrH have no features (for vibrational transitions) in the mid-IR region where the LiCl feature is located. Although the global opacity is expected to be changed overall using these new line lists, for the purpose and wavelength window of this paper the use of the line lists of Phillips & Davis (1993) and R. Freedman is appropriate. The models account for equilibrium formation of dust and condensates and include grain opacities for 40 species. In this paper we only consider the so-called “AMES-cond” models in which the dust particles have sunk below the atmosphere from the layers in which they originally formed. As demonstrated in Allard et al. (2001) this limiting case is appropriate for T dwarfs which are discussed in this paper. We stress that large uncertainties persist in the water opacities for parts of the temperature range of this work (Allard et al. 2000).

In addition to the opacity sources listed above and in Allard et al. (2001, and references therein) the new LiCl line list presented in this paper has been added to our opacity database. In order to assess the effects of the new LiCl line data, we compare spectra calculated with and without this opacity source. The models used in the following discussion were all iterated

to convergence for the parameters indicated. The high resolution spectra which have the individual opacity sources selected are calculated on top of the models. The LiCl line opacity data turned out to be too weak to influence the temperature structure of the atmosphere. The models have solar abundances with the non-depleted lithium abundance of $\log(n_{\text{Li}})=3.31$.

We calculated models with $\log(g)=3.0, 4.0$ and 5.0 and effective temperatures of 900 K , 1200 K and 1500 K which are typical parameters of old ($\log(g) = 5.0, > 1\text{ Gyr}$) to young ($\log(g) = 3.0, \simeq 100\text{ Myrs}$) T dwarfs. This parameter region turned out to be the one showing the strongest LiCl features. As can be seen in Figure 2 the effect of LiCl is strongest for $T_{\text{eff}}=1200\text{ K}$ and $\log(g)=3.0$ in the IR around the fundamental vibrational band origin at $15.8\text{ }\mu\text{m}$ and the relative flux difference is typically less than 20% overall. The general strength of the LiCl absorption warrants inclusion in model calculations, but the lack of a distinct feature will make it hard to detect in an observed spectrum which is dominated by water absorption. However, the model parameters $T_{\text{eff}}=1200\text{ K}$ and $\log(g)=3.0$ are particularly interesting since these are parameters typical for very young (and hence very bright) mid to early T dwarfs.

4. Conclusion

Using an accurate hybrid potential and fully quantum-mechanical techniques, we have constructed a comprehensive and complete theoretical line list of spectroscopic accuracy for the $X\ ^1\Sigma^+$ electronic ground state of $^7\text{Li}^{35}\text{Cl}$. Although LiCl appears to be a dominant Li-bearing gas over an extended domain of the (T, P) diagram in cool dwarf atmospheres, synthetic spectra calculations with the stellar atmosphere code PHOENIX suggest that flux differences resulting from the incorporation of this new line list are less than 20% for parameters typical of young to old T dwarfs. The strongest signature of LiCl for $T_{\text{eff}}=1200\text{ K}$ and $\log(g)=3.0$ appears in the vicinity of the fundamental vibrational band origin at $15.8\text{ }\mu\text{m}$, where the spectrum is dominated by water absorption. The current results suggest that it will be difficult to measure the full inventory of elemental lithium in T dwarfs after it is repositied into molecular species.

This work was supported by NASA grants NAG5-8425, NAG5-9222, and NAG5-10551 as well as NASA/JPL grant 961582, and in part by NSF grants AST-9720704 and AST-0086246 (and a grant to the Institute for Theoretical Atomic, Molecular & Optical Physics, Harvard-Smithsonian CfA). Some of the calculations were performed on the IBM SP “Blue Horizon” of the San Diego Supercomputer Center, with support from the NSF, and on the IBM SP of NERSC with support from the DoE. This work also was supported in part by the

Pôle Scientifique de Modélisation Numérique at ENS-Lyon. P.F.W. acknowledges ITAMP at Harvard University and SAO for travel support.

REFERENCES

- Allard, F., Hauschildt, P. H., Alexander, D. R., Tamanai, A., & Schweitzer, A. 2001, *ApJ*, 556, 357
- Allard, F., Hauschildt, P. H., & Schweitzer, A. 2000, *ApJ*, 539, 366
- Barrado y Navascués, D., Stauffer, J. R., & Patten, B. M. 1999, *ApJ*, 522, L53
- Basri, G., Marcy, G. W., & Graham, J. R. 1996, *ApJ*, 458, 600
- Brewer, L., & Brackett, E. 1961, *Chem. Rev.*, 61, 425
- Bulewicz, E. M., Phillips, L. F., & Sugden, T. M. 1961, *Trans. Faraday Soc.*, 57, 921
- Burrows, A., Marley, M. S., & Sharp, C. M. 2000, *ApJ*, 531, 438
- Burrows, A., Ram, R. S., Bernath, P., Sharp, C. M., & Milsom, J. A. 2002, *ApJ*, 577, 986
- Chabrier, G., & Baraffe, I. 1997, *A&A*, 327, 1039
- Cooley, J. W. 1961, *Math. Computation*, 15, 363
- Dulick, M., Bauschlicher, C. W., Jr., Burrows, A., Sharp, C. M., Ram, R. S., & Bernath, P. 2003, *ApJ*, 594, 651
- Hauschildt, P. H., & Baron, E. 1999, *J. Comput. App. Math.* 102, 41
- Huber, K. P., & Herzberg, G. 1979, *Molecular Spectra and Molecular Structure, Vol. IV, Constants of Diatomic Molecules* (New York: Van Nostrand Reinhold)
- Jones, H., & Lindenmayer, J. 1987, *Chem. Phys. Lett.*, 135, 189
- Lodders, K. 1999, *ApJ*, 519, 793
- Ogilvie, J. F. 1992, *Spectrosc. Lett.*, 25, 1341
- Partridge, H., & Schwenke, D. W. 1997, *J. Chem. Phys.*, 106, 4618
- Phillips, J. G., & Davis S. P. 1993, *ApJ*, 409, 860

- Rebolo, R., Martin, E. L., & Magazzu, A. 1992, *ApJ*, 389, L83
- Schwenke, D. W. 1998, *Chemistry and Physics of Molecules and Grains in Space*, Faraday Discussion, 109, 321
- Skory, S. S., Weck, P. F., Stancil, P. C., & Kirby, K. 2003, *ApJ*, 148, 599
- Thompson, G. A., Maki, A. G., Olson, W. B., & Weber, A. 1987, *J. Mol. Spectrosc.*, 124, 130
- Weck, P. F., Schweitzer, A., Stancil, P. C., Hauschildt, P. H., & Kirby, K. 2003a, *ApJ*, 582, 1059
- Weck, P. F., Schweitzer, A., Stancil, P. C., Hauschildt, P. H., & Kirby, K. 2003b, *ApJ*, 584, 459
- Weck, P. F., Stancil, P. C., & Kirby, K. 2003c, *J. Chem. Phys.*, 118, 9997
- Weck, P. F., Kirby, K., & Stancil, P. C. 2004, *J. Chem. Phys.*, 120, 4216

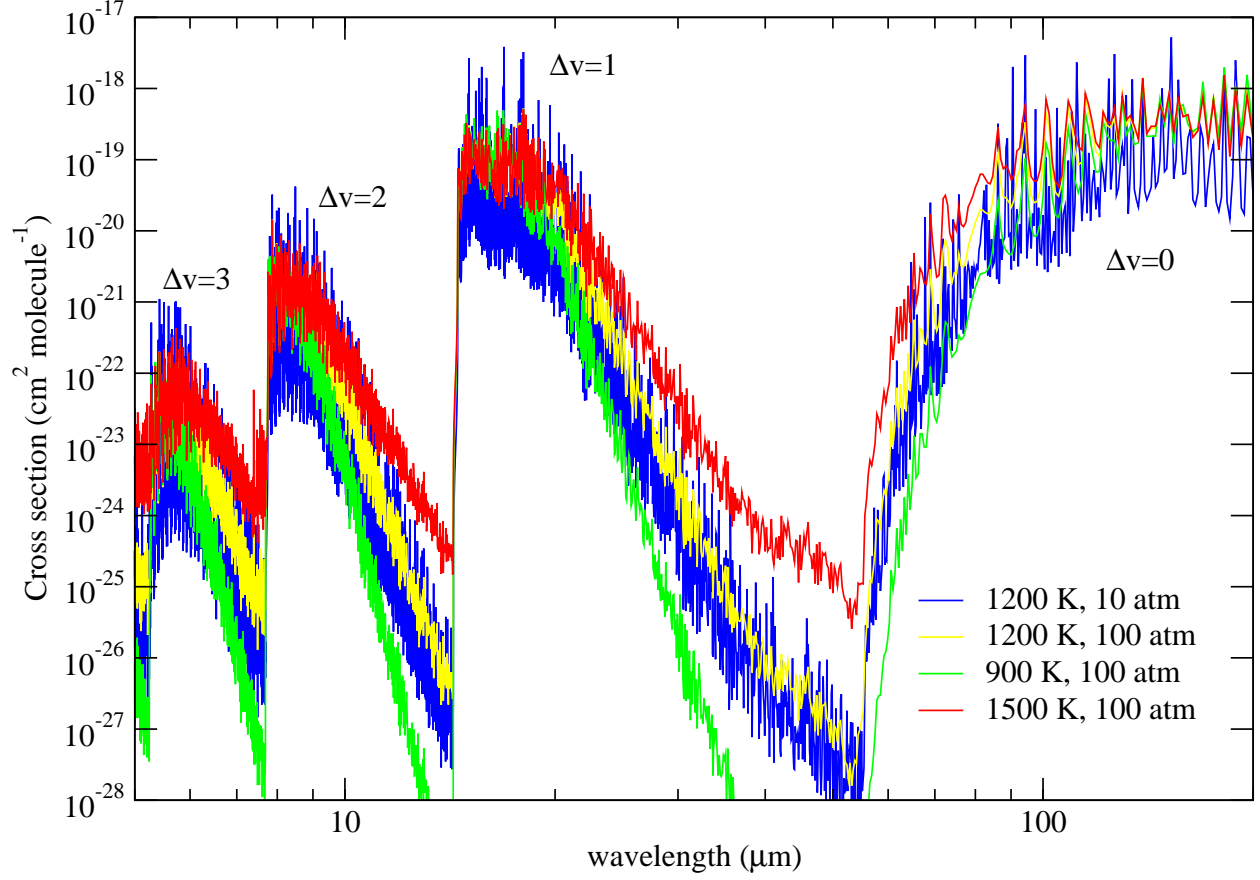


Fig. 1.— Representative absorption cross sections for the $X^1\Sigma^+$ state of LiCl. 1200 K and 10 atm (blue). 900 (green), 1200 (yellow), and 1500 K (red), all at 100 atm. The opacity for the fundamental and first two overtone vibrational bands as well as a portion of the pure rotational band are shown.

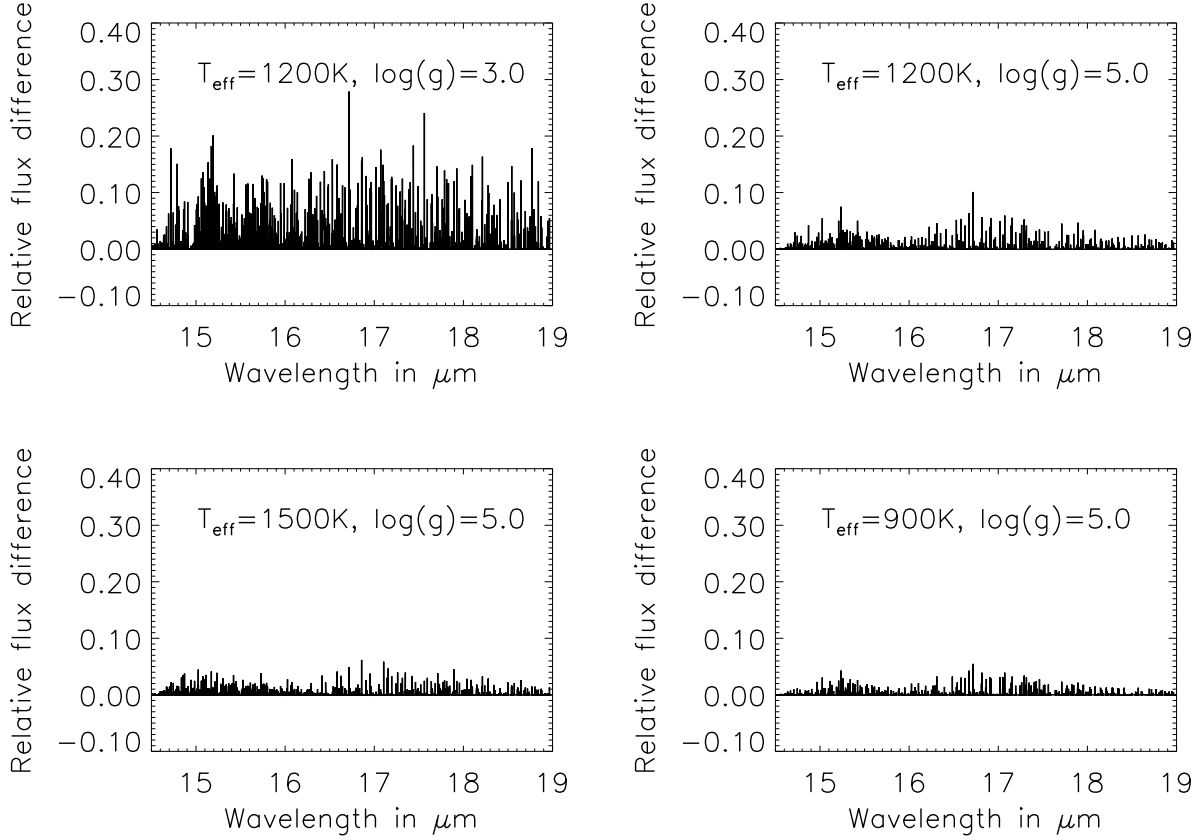


Fig. 2.— Relative flux difference for brown dwarf model spectra with and without the present LiCl line opacity data for $T_{\text{eff}} = 900 - 1500\text{ K}$, $\log(g) = 3.0 - 5.0$ and solar abundances. The relative flux difference is defined here as $(F_0 - F_{\text{LiCl}})/F_0$ where F_0 is the flux calculated with no LiCl absorption in our models and F_{LiCl} is the flux including our new LiCl line list. The positive differences mean that there is less flux in the LiCl bands when including LiCl absorption data. The largest relative flux difference values correspond to the maximum effect of the LiCl absorption.

Table 1. Line Oscillator Strengths and
Transition Energies for Transitions in the
 $X^1\Sigma^+$ state

Band	Line	$f_{v',J',v'',J''}^a$	Transition Energy (cm ⁻¹)		
			Theory ^a	Expt. ^b	ΔE^c
1 \leftarrow 0	R(7)	1.26217(-5)	644.64	644.7380	0.0980
	R(10)	1.21968(-5)	648.35	648.4665	0.1165
	R(16)	1.16041(-5)	655.30	655.4703	0.1703
	R(19)	1.13577(-5)	658.55	658.7408	0.1908
	R(22)	1.11270(-5)	661.64	661.8543	0.2143
	R(26)	1.08349(-5)	665.53	665.7600	0.2300
	R(34)	1.02818(-5)	672.44	672.7089	0.2689
	R(49)	9.30016(-6)	682.23	682.5450	0.3150
	R(50)	9.23624(-6)	682.73	683.0491	0.3191
	R(58)	8.72963(-6)	686.06	686.3802	0.3208
2 \leftarrow 1	R(1)	3.25145(-5)	628.00	628.0418	0.0418
	R(6)	2.55717(-5)	634.51	634.5921	0.0821
	R(12)	2.38987(-5)	641.78	641.9116	0.1316
	R(18)	2.28181(-5)	648.45	648.6304	0.1804
	R(23)	2.20447(-5)	653.55	653.7615	0.2115
	R(25)	2.17516(-5)	655.47	655.6910	0.2210
	R(28)	2.13235(-5)	658.21	658.4520	0.2420
	R(32)	2.07686(-5)	661.62	661.8852	0.2652
	R(36)	2.02270(-5)	664.75	665.0280	0.2780
	R(37)	2.00932(-5)	665.49	665.7710	0.2810
	R(48)	1.86527(-5)	672.38	672.6855	0.3055
3 \leftarrow 2	R(5)	3.89879(-5)	624.51	624.5800	0.0700
	R(13)	3.54663(-5)	634.09	634.2288	0.1388
	R(16)	3.46439(-5)	637.42	637.5746	0.1546
	R(20)	3.36623(-5)	641.61	641.8000	0.1900
	R(23)	3.29764(-5)	644.58	644.7908	0.2108
	R(27)	3.21029(-5)	648.30	648.5320	0.2320

Table 1—Continued

Band	Line	$f_{v'J',v''J''}^a$	Transition Energy (cm ⁻¹)		
			Theory ^a	Expt. ^b	ΔE^c
	R(40)	2.94364(-5)	658.45	658.7343	0.2843
	R(45)	2.84505(-5)	661.54	661.8405	0.3005
	R(46)	2.82550(-5)	662.10	662.4058	0.3058
	R(51)	2.72851(-5)	664.64	664.9493	0.3093
	R(52)	2.70924(-5)	665.09	665.3980	0.3080
4 ← 3	R(12)	4.75816(-5)	624.26	624.3715	0.1115
	R(15)	4.64316(-5)	627.60	627.7262	0.1262
	R(25)	4.32566(-5)	637.63	637.8264	0.1964
	R(33)	4.09981(-5)	644.42	644.6672	0.2472
	R(38)	3.96417(-5)	648.10	648.3652	0.2652
	R(50)	3.64842(-5)	655.09	655.3840	0.2940
	R(58)	3.44306(-5)	658.27	658.5725	0.3025
5 ← 4	R(17)	5.70297(-5)	621.13	621.2291	0.0991
	R(20)	6.70073(-5)	624.18	624.3003	0.1203
	R(32)	5.14267(-5)	634.85	635.0536	0.2036
	R(47)	4.63923(-5)	644.66	644.9326	0.2726
	R(55)	4.37976(-5)	648.23	648.5196	0.2896

^aThis work.

^bJones & Lindenmayer (1987).

^c $\Delta E = E_{Expt.} - E_{Theory}$